Syntheses, Structures, and Properties of Tricarbonyl Rhenium(I) Heteronuclear Complexes with a New Bridging Ligand Containing Coupled Bis(2-pyridyl) and 1,2-Dithiolene Units

Wei Liu, Ru Wang, Xin-Hui Zhou, Jing-Lin Zuo,* and Xiao-Zeng You

Coordination Chemistry Institute and the State Key Laboratory of Coordination Chemistry, School of Chemistry and Chemical Engineering, Nanjing University, Nanjing 210093, People's Republic of China

Received July 31, 2007

A new type of polypyridine ligand containing coupled bis(2-pyridyl) and cyanoethylthio-protected dithiolene, 4,5-bis(2-cyanoethylthio)-2-bis(2-pyridyl)methylene-1,3-dithiole (BPyDT(SCH_2CH_2CN)$_2$, **3**), two mononuclear complexes, BrRe(CO)$_3$(BPyDT(SCH_2CH_2CN)$_2$) (**4**) and BPyDTS_2Pt(dbbpy) (**7**), and one homodinuclear complex, BPyDT($SAuPPh_3$)$_2$ (**5**), have been synthesized and characterized. With the deprotected polypyridine ligand BPyDTS_2^{2-} as the bridging unit, one tricarbonyl rhenium(I) heterotrinuclear complex, ClRe(CO)$_3$(BPyDT($SAuPPh_3$)$_2$) (**6**), and one heterodinuclear complex, ClRe(CO)$_3$(BPyDTS_2Pt(dbbpy)) (**8**, dbbpy = 4,4′-di-*tert*-butyl-2,2′-bipyridine), have been studied. The structures of all these compounds have been determined by X-ray crystallography. UV–vis studies have been carried out for them, showing distinct electronic absorptions. Compounds **3**–**6** exhibit blue to red luminescence in CH_2Cl_2 solution at room temperature. Ground-state electronic structures for **3**–**8** have been analyzed by the B3LYP calculations.

Introduction

Since originally delivered by Wrighton and Morse,[1] rhenium(I) complexes of the $[ReL(CO)_3]^+$ (L = polypyridine) type have been expanded greatly. Due to their abundant photophysical and photochemical properties, these rhenium(I) complexes have attracted growing interest.[2–7] Another impetus for the prosperous development is that they are chemically stable and can be easily synthesized and functionalized to obtain novel properties. A number of rules for synthetic guidance in this field have been outlined.[3]

Chart 1

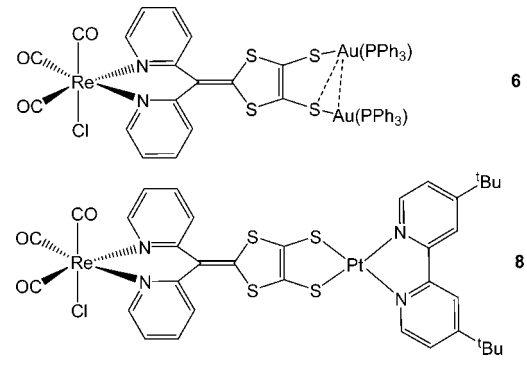

During the past several years, much attention has been focused on heterometallic rhenium(I) systems,[4–7] since their spectroscopic properties are not easy to predict and analogize from the structurally building units. Complexes with a 1,2-dithiolene moiety have been studied extensively for exploring multifunctional molecular materials.[8] With our experience in the multisulfur systems, recently we are endeavoring to utilize their electron-rich feature to serve as versatile bridging ligands or building blocks for combining many fascinating units.[9] In this paper, we designed and synthesized a new type of

* To whom correspondence should be addressed. E-mail: zuojl@nju.edu.cn. Fax: +86-25-83314502.

(1) Wrighton, M.; Morse, D. L. *J. Am. Chem. Soc.* **1974**, *96*, 998.

(2) (a) Lo, K. K. W.; Tsang, K. H. K.; Zhu, N. *Organometallics* **2006**, *25*, 3220. (b) Busby, M.; Matousek, P.; Towrie, M.; Clark, I. P.; Motevalli, M.; Hartl, F.; Vlček, A., Jr. *Inorg. Chem.* **2004**, *43*, 4523. (c) Wei, L.; Babich, J. W.; Ouellette, W.; Zubieta, J. *Inorg. Chem.* **2006**, *45*, 3057. (d) Wang, K. Z.; Huang, L.; Gao, L. H.; Jin, L. P.; Huang, C. H. *Inorg. Chem.* **2002**, *41*, 3353. (e) Yam, V. W. W.; Ko, C. C.; Zhu, N. *J. Am. Chem. Soc.* **2004**, *126*, 12734.

(3) (a) Koike, K.; Okoshi, N.; Hori, H.; Takeuchi, K.; Ishitani, O.; Tsubaki, H.; Clark, I. P.; George, M. W.; Johnson, F. P. A.; Turner, J. J. *J. Am. Chem. Soc.* **2002**, *124*, 11448. (b) Tsubaki, H.; Sekine, A.; Ohashi, Y.; Koike, K.; Takeda, H.; Ishitani, O. *J. Am. Chem. Soc.* **2005**, *127*, 15544. (c) Marti, N.; Spingler, B.; Breher, F.; Schibli, R. *Inorg. Chem.* **2005**, *44*, 6082. (d) de Silva, A. P.; Gunaratne, N.; Gunnlaugsson, T.; Huxley, A. J. M.; McCoy, C. P.; Rademacher, J. T.; Rice, T. E. *Chem. Rev.* **1997**, *97*, 1515. (e) Stufkens, D. J.; Vlček, A., Jr *Coord. Chem. Rev.* **1998**, *117*, 127. (f) Lees, A. J. *Chem. Rev.* **1987**, *87*, 711, and further references therein.

(4) (a) Pomestchenko, I. E.; Polyansky, D. E.; Castellano, F. N. *Inorg. Chem.* **2005**, *44*, 3412. (b) Lam, S. C. F.; Yam, V. W. W.; Wong, K. M. C.; Cheng, E. C. C.; Zhu, N. *Organometallics* **2005**, *24*, 4298. (c) Gabrielsson, A.; Hartl, F.; Zhang, H.; Lindsay Smith, J. R.; Towrie, M.; Vlček, A., Jr.; Perutz, R. N. *J. Am. Chem. Soc.* **2006**, *128*, 4253. (d) Coe, B. J.; Curati, N. R. M.; Fitzgerald, E. C.; Coles, S. J.; Horton, P. N.; Light, M. E.; Hursthouse, M. B. *Organometallics* **2007**, *26*, 2318.

(5) (a) Reger, D. L.; Watson, R. P.; Smith, M. D.; Pellechia, P. J. *Organometallics* **2005**, *24*, 1544. (b) Wei, Q. H.; Yin, G. Q.; Zhang, L. Y.; Chen, Z. N. *Inorg. Chem.* **2006**, *45*, 10371. (c) Cattaneo, M.; Fagalde, F.; Katz, N. E. *Inorg. Chem.* **2006**, *45*, 6884. (d) de Wolf, P.; Waywell, P.; Hanson, M.; Heath, S. L.; Meijer, A. J. H. M.; Teat, S. J.; Thomas, J. A. *Chem.*−*Eur. J.* **2006**, *12*, 2188.

(6) (a) Wong, K. M. C.; Lam, S. C. F.; Ko, C. C.; Zhu, N.; Yam, V. W. W.; Roué, S.; Lapinte, C.; Fathallah, S.; Costuas, K.; Kahlal, S.; Halet, J. F. *Inorg. Chem.* **2003**, *42*, 7086. (b) Azócar, M. I.; Mikelsons, L.; Ferraudi, G.; Moya, S.; Guerrero, J.; Aguirre, P.; Martinez, C. *Organometallics* **2004**, *23*, 5967. (c) Yam, V. W. W.; Lo, W. Y.; Lam, C. H.; Fung, W. K. M.; Wong, K. M. C.; Lau, V. C. Y.; Zhu, N. *Coord. Chem. Rev.* **2003**, *245*, 39.

(7) (a) Kennedy, F.; Shavaleev, N. M.; Koullourou, T.; Bell, Z. R.; Jeffery, J. C.; Faulkner, S.; Ward, M. D. *J. Chem. Soc., Dalton Trans.* **2007**, 1492. (b) Shavaleev, N. M.; Accorsi, G.; Virgili, D.; Bell, Z. R.; Lazarides, T.; Calogero, G.; Armaroli, N.; Ward, M. D. *Inorg. Chem.* **2005**, *44*, 61. (c) Kühn, F. E.; Zuo, J. L.; Fabrizi de Biani, F.; Santos, A. M.; Zhang, Y.; Zhao, J.; Sandulachea, A.; Herdtweck, E. *New J. Chem.* **2004**, *28*, 43.

10.1021/om700776s CCC: $40.75
Publication on Web 12/19/2007

Scheme 1. Synthetic Routes to 3–8

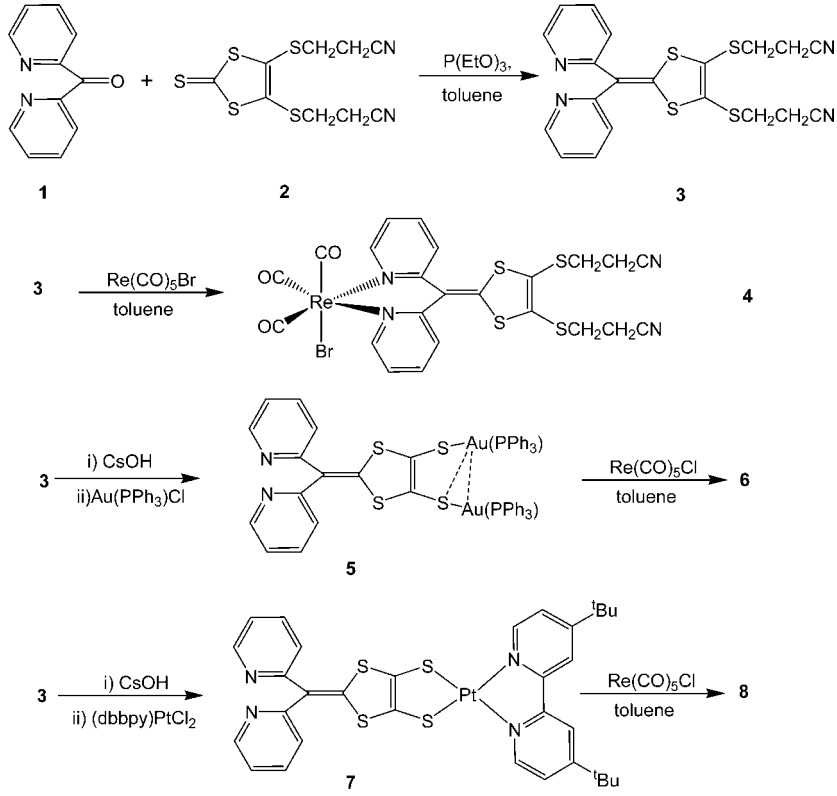

polypyridine, $BPyDTS_2^{2-}$, as the bridging ligand. The new multidentate ligand provides two types of chelating sites, bis(2-pyridyl) and 1,2-ene-dithiolato units, which can bind homo- or heterometal ions together to form multinuclear complexes. Based on this, two novel tricarbonyl rhenium(I) complexes containing heterometals have been synthesized (Chart 1). Herein, the preparation, spectroscopy, and crystallographic analyses of these complexes are described.

Experimental Section

General Considerations. Schlenk techniques were used in carrying out manipulations under a N_2 atmosphere. The IR spectra were taken on a Vector22 Bruker spectrophotometer (400–4000 cm^{-1}) with KBr pellets. Absorption spectra were measured on a UV-3100 spectrophotometer. Elemental analyses for C, H, and N were performed on a Perkin-Elmer 240C analyzer. Florescence measurements were carried out on AMINCO Bowman Series 2 luminescence spectrometer in a 1 cm quartz cell. NMR spectra were measured on a Bruker AM 500 spectrometer. Mass spectra were determined with an Autoflex ^{II}TM instrument for MALDI-TOF-MS. The precursors (dbbpy)$PtCl_2$ (dbbpy = 4,4′-di-*tert*-butyl-2,2′-bipyridine) and $AuPPh_3Cl$ were prepared by the literature methods.[10,11] The compound 4,5-bis(2-cyanoethylthio)-1,3-dithiole-2-thione (**2**) was synthesized as described in the literature.[12] All solvents and chemicals were purchased from commercial sources and used as received.

4,5-Bis(2-cyanoethylthio)-2-bis(2-pyridyl)methylene-1,3-dithiole (3, BPyDT(SCH_2CH_2CN)$_2$). Under a nitrogen atmosphere, a mixture of di(2-pyridyl)ketone (**1**) (921 mg, 5 mmol) and **2** (1.522 g, 5 mmol) was dissolved in 15 mL of toluene. After addition of 5 mL of $P(OEt)_3$, the reaction mixture was refluxed at 110 °C for 4 h. Then the solution was cooled to room temperature. After evaporation of solvents under reduced pressure, a greenish-yellow precipitate was filtrated and washed with Et_2O. After decolorization with activated carbon, yellow solids of **3** were obtained. Needle-like crystals were obtained from CH_2Cl_2/Et_2O. Yield: 967 mg (44%). IR (KBr, cm^{-1}): 2243 ($\nu_{C\equiv N}$), 1574, 1526, 1457, 1448, 1281, 781. ^{1}H NMR (500 MHz, $CDCl_3$, ppm): δ 8.77 (d, 2H, J = 4.8, $BPyH^{6,6'}$), 7.71 (t, 2H, $BPyH^{4,4'}$), 7.22 (t, 2H, $BPyH^{3,3'}$), 7.14 (d, 2H, J = 8.0, $BPyH^{5,5'}$), 3.11(t, 4H, $-SCH_2CH_2CN$), 2.73(t, 4H, $-SCH_2CH_2CN$). MS (MALDI-TOF): m/z 441.1 (M^+). Anal. Calcd for $C_{20}H_{16}N_4S_4$: C, 54.52; H, 3.66; N, 12.72. Found: C, 54.39; H, 3.58; N, 12.62.

BrRe(CO)$_3$(BPyDT(SCH_2CH_2CN)$_2$) (4). Compound **4** was synthesized under N_2, by refluxing $Re(CO)_5Br$ (41 mg, 0.1 mmol) and **3** (44 mg, 0.1 mmol) in 10 mL of toluene for 50 min. After evaporation of solvents under reduced pressure, a crude product was obtained. Purification was achieved by a short alumina column using CH_2Cl_2 as the eluent. Yellow crystals were obtained from diffusion of Et_2O into $CHCl_3$ solutions. Yield: 64 mg (63%). IR (KBr, cm^{-1}): 2247 ($\nu_{C\equiv N}$), 2022, 1908, 1896 ($\nu_{C\equiv O}$). ^{1}H NMR (500 MHz, $CDCl_3$, ppm): δ 9.29 (d, 2H, J = 5.5, $BPyH^{6,6'}$), 7.92–7.97 (m, 2H, $BPyH^{4,4'}$), 7.68 (d, 2H, J = 7.5, $BPyH^{3,3'}$), 7.42 (t, 2H, $BPyH^{5,5'}$), 3.13–3.18 (m, 2H, SCH_2CH_2CN), 2.95–3.01 (m, 2H, $-SCH_2CH_2CN$), 2.63–2.74 (m, 4H, $-SCH_2CH_2CN$). MS (MALDI-TOF): m/z 763.0 [M − CO]$^+$, 711.0 [M − Br]$^+$. Anal. Calcd for

(8) (a) Ouahab, L. *Coord. Chem. Rev.* **1998**, *178–180*, 1501. (b) Segura, J.; Martín, N. *Angew. Chem., Int. Ed.* **2001**, *40*, 1372. (c) Robertson, N.; Cronin, L. *Coord. Chem. Rev.* **2002**, *227*, 93. (d) Coronado, E.; Day, P. *Chem. Rev.* **2004**, *104*, 5419. (e) Rovira, C. *Chem. Rev.* **2004**, *104*, 5289. (f) Baudron, S. A.; Hosseini, M. W *Inorg. Chem.* **2006**, *45*, 5260, and further references therein.

(9) (a) Ji, Y.; Zhang, R.; Li, Y. J.; Li, Y. Z.; Zuo, J. L.; You, X. Z. *Inorg. Chem.* **2007**, *46*, 866. (b) Wen, H. R.; Li, C. H.; Song, Y.; Zuo, J. L.; Zhang, B.; You, X. Z. *Inorg. Chem.* **2007**, *46*, 6837.

(10) Juris, A.; Balzani, V.; Barigelletti, F.; Campagna, S.; Belser, P.; Von Zelewsky, A. *Coord. Chem. Rev.* **1988**, *84*, 85.

(11) McAuliffe, C. A; Parish, R. V.; Randall, P. D. *J. Chem. Soc., Dalton Trans.* **1979**, 1730.

(12) Kumasaki, M.; Tanaka, H.; Kobayashi, A. *J. Mater. Chem.* **1998**, *8*, 301.

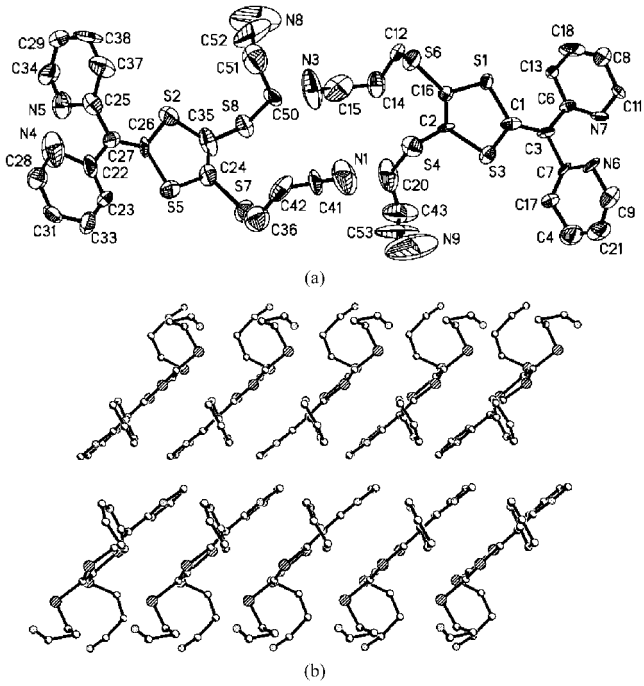

Figure 1. (a) ORTEP view of ligand **3** with the atom-numbering scheme (hydrogen atoms are omitted for clarity, and ellipsoids are drawn at the 50% probability level). (b) Packing diagram of **3** viewed along the *b* axis (hydrogen atoms omitted).

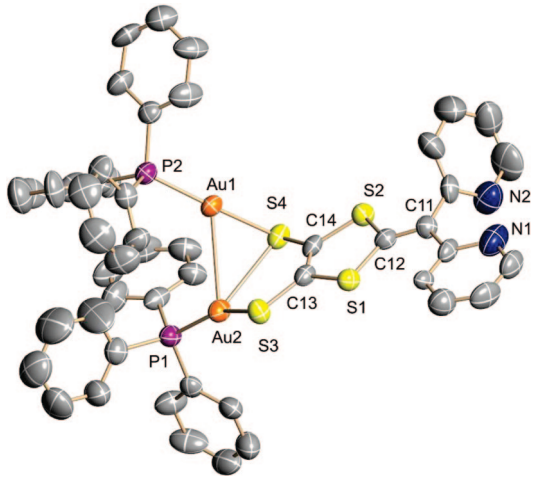

Figure 2. ORTEP view of complex **5** with the atom-numbering scheme. Hydrogen atoms are omitted for clarity. Ellipsoids are drawn at the 50% probability level.

$C_{25}H_{18}BrCl_6N_4O_3ReS_4$: C, 29.17; H, 1.76; N, 5.44. Found: C, 29.09; H, 1.85; N, 5.35.

BPyDT(SAuPPh$_3$)$_2$ (5). Under a nitrogen atmosphere, to a solution of **3** (176 mg, 0.4 mmol) in THF (15 mL) was added dropwise a solution of CsOH·H_2O (134 mg, 0.8 mmol) in methanol (5 mL). The mixture was stirred for an additional 30 min, and a solution of $AuPPh_3Cl$ (395 mg, 0.8 mmol) in 15 mL of CH_2Cl_2 was added. The reaction mixture was further stirred for 3 h at room temperature. Then the reaction mixture was evaporated and extracted with CH_2Cl_2, and the combined organic extracts were washed with water and dried over Na_2SO_4. The solvent was removed, and pure product was obtained after chromatography by using CH_2Cl_2/Et_2O (v/v, 1:1) as eluent. Yield: 300 mg (60%). Yellow crystals were obtained from CH_2Cl_2/Et_2O. IR (KBr, cm^{-1}): 2850, 2364, 2344, 1580, 1562, 1478, 1450, 1434, 1422, 1099, 744, 691, 535, 498, 465; ^{1}H NMR (500 MHz, $CDCl_3$, ppm): δ 7.51 (d, 38H, J = 17.5, aromatic and pyridine). MS (MALDI-TOF): m/z 1250.3 (M^+). Anal. Calcd for $C_{51}H_{45}Au_2Cl_2N_2O_{2.5}P_2S_4$: C, 44.36; H, 3.28; N, 2.03. Found: C, 44.48; H, 3.19; N, 2.11.

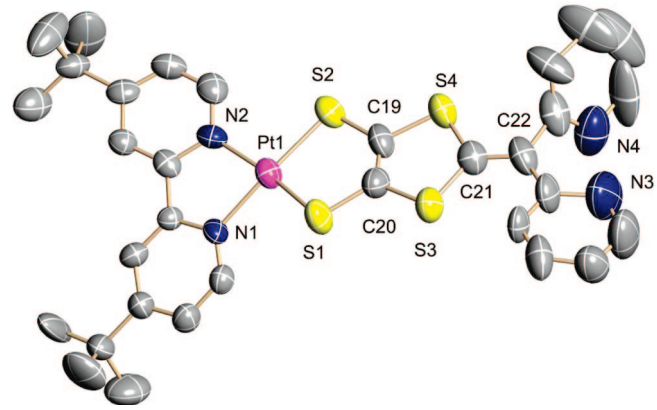

Figure 3. ORTEP view of complex **7** with the atom-numbering scheme. Hydrogen atoms are omitted for clarity. Ellipsoids are drawn at the 50% probability level.

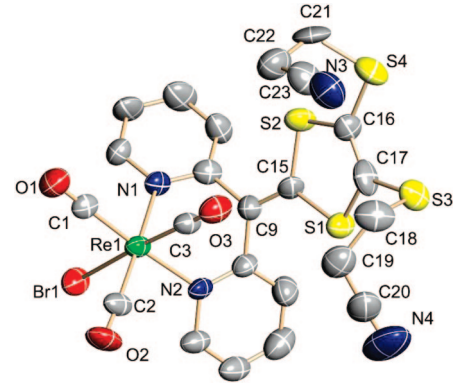

Figure 4. ORTEP view of complex **4** with the atom-numbering scheme. Hydrogen atoms are omitted for clarity. Ellipsoids are drawn at the 30% probability level.

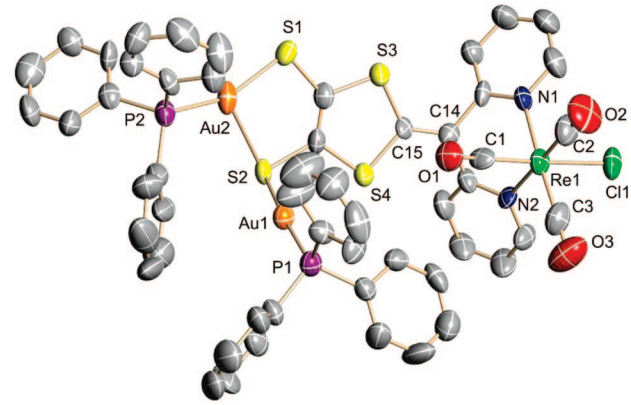

Figure 5. ORTEP view of complex **6** with the atom-numbering scheme. Hydrogen atoms are omitted for clarity. Ellipsoids are drawn at the 50% probability level.

ClRe(CO)$_3$(BPyDT(SAuPPh$_3$)$_2$) (6). Under a nitrogen atmosphere, a mixture of $Re(CO)_5Cl$ (22 mg, 0.06 mmol) and **5** (75 mg, 0.06 mmol) was refluxed in 8 mL of toluene for 40 min. The solvent was removed, and pure product was obtained after chromatography by using CH_2Cl_2 as eluent (alumina). Orange crystals were obtained from CH_2Cl_2/Et_2O. Yield: 65 mg (63%). IR (KBr, cm^{-1}): 2015, 1906, 1884 ($\nu_{C\equiv O}$). ^{1}H NMR (500 MHz, $CDCl_3$, ppm): δ 7.34–7.99 (m, 38H, aromatic and pyridine). MS (MALDI-

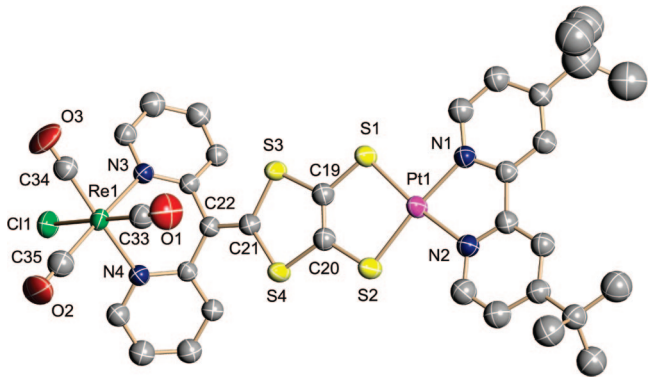

Figure 6. ORTEP view of complex **8** with the atom-numbering scheme. Hydrogen atoms are omitted for clarity. Ellipsoids are drawn at the 50% probability level.

TOF): *m*/*z* 1521.4 $[M - Cl]^+$, 1250.4 $[M - 3CO - Cl - Re]^+$. Anal. Calcd for $C_{55}H_{42}Au_2Cl_5N_2O_3P_2ReS_4$: C, 38.26; H, 2.45; N, 1.62. Found: C, 38.17; H, 2.49; N, 1.51.

BPyDTS$_2$Pt(dbbpy) (7). Under a nitrogen atmosphere, to a solution of **3** (97 mg, 0.22 mmol) in THF (8 mL) was added dropwise a solution of $CsOH \cdot H_2O$ (74 mg, 0.44 mmol) in methanol (5 mL). The mixture was stirred for an additional 30 min, and a suspension of (dbbpy)$PtCl_2$ (118 mg, 0.22 mmol) in 15 mL of CH_3OH was added. The reaction mixture was further stirred for 1 h at room temperature. Then the reaction mixture was evaporated to give the crude product. Green crystals were obtained from $CHCl_3$/Et_2O. Yield: 123 mg (71%). IR (KBr, cm^{-1}): 2850, 2364, 2344, 1580, 1562, 1478, 1450, 1434, 1422, 1099, 744, 691, 535, 498, 465. ^{1}H NMR (500 MHz, $CDCl_3$, ppm): δ 9.57 (d, 2H, J = 6.4, BPyH$^{6,6'}$), 7.91 (d, 6H, J = 11.3, BPyH$^{4,4'}$, dbbpyH$^{3,3'}$, dbbpyH$^{6,6'}$), 7.53 (d, 2H, J = 6.2, BPyH$^{3,3'}$), 7.44 (d, 4H, J = 8.0, BPyH$^{5,5'}$, dbbpyH$^{5,5'}$), 1.46 (d, 18H, J = 6.8, ^{t}Bu). MS (MALDI-TOF): *m*/*z* 795.6 (M^+). Anal. Calcd for $C_{32}H_{32}N_4PtS_4$: C, 48.29; H, 4.05; N, 7.04. Found: C, 48.15; H, 4.18; N, 7.14.

ClRe(CO)$_3$(BPyDTS$_2$Pt(dbbpy)) (8). Under a nitrogen atmosphere, a mixture of $Re(CO)_5Cl$ (36 mg, 0.1 mmol) and **7** (80 mg, 0.1 mmol) was refluxed in 8 mL of toluene for 40 min. The solvent was removed to give the product. The violet crystals were obtained

Table 1. Crystallographic Data for Compounds 3, 5, and 7

	3	**5**$\cdot CH_2Cl_2 \cdot 2.5H_2O$	**7**
empirical formula	$C_{20}H_{16}N_4S_4$	$C_{51}H_{45}Au_2Cl_2N_2O_{2.50}P_2S_4$	$C_{32}H_{32}N_4PtS_4$
M_r	440.61	1380.90	795.95
cryst syst	monoclinic	monoclinic	monoclinic
space group	$P2_1$	$P2_1/n$	$P2_1/c$
a (Å)	5.195(5)	17.174(9)	18.866(5)
b (Å)	9.580(9)	14.140(7)	10.910(3)
c (Å)	41.29(4)	22.720(12)	15.820(4)
α (deg)	90.00	90.00	90.00
β (deg)	90.000(18)	93.788(10)	104.639(5)
γ (deg)	90.00	90.00	90.00
V (Å^3)	2055(3)	5505(5)	3150.5(15)
Z	4	4	4
ρ_c (g cm^{-3})	1.424(2)	1.666	1.678
F(000)	912.0	2684	1576
T/K	293(2)	293(2)	293(2)
μ(Mo Kα) (mm^{-1})	0.476	5.670	4.748
index ranges	$-6 \le h \le 6$	$-17 \le h \le 22$	$-22 \le h \le 22$
	$-11 \le k \le 8$	$-18 \le k \le 18$	$-11 \le k \le 12$
	$-40 \le l \le 48$	$-29 \le l \le 25$	$-9 \le l \le 18$
GOF (F^2)	1.052	1.046	0.988
$R_1{}^a$, $wR_2{}^b$ ($I > 2\sigma(I)$)	0.0857, 0.2278	0.0566, 0.1509	0.0642, 0.1604
$R_1{}^a$, $wR_2{}^b$ (all data)	0.0944, 0.2410	0.0954, 0.1669	0.0909, 0.1700

^{a} $R_1 = \sum C| - |F_c/\sum F_o|$. ^{b} $R_2 = [\sum w(F_o^2 - F_c^2)^2/\sum w(F_o^2)]^{1/2}$.

Table 2. Crystallographic Data for Complexes 4, 6, and 8

	4$\cdot 2CHCl_3$	**6**$\cdot 2CH_2Cl_2$	**8**$\cdot$DMF
empirical formula	$C_{25}H_{18}BrCl_6N_4O_3ReS_4$	$C_{55}H_{42}Au_2Cl_5N_2O_3P_2ReS_4$	$C_{38}H_{39}ClN_5O_4PtReS_4$
M_r	1029.48	1726.47	1174.72
cryst syst	monoclinic	triclinic	triclinic
space group	$P2_1/c$	$P\bar{1}$	$P\bar{1}$
a (Å)	17.761(8)	12.413(2)	8.9503(17)
b (Å)	10.191(4)	15.205(3)	13.158(3)
c (Å)	22.264(7)	17.430(3)	17.986(3)
α (deg)	90.00	103.993(4)	100.325(3)
β (deg)	116.61(3)	104.478(4)	94.305(3)
γ (deg)	90.00	99.802(4)	98.211(4)
V (Å^3)	3603(2)	2996.0(10)	2051.5(7)
Z	4	2	2
ρ_c (g cm^{-3})	1.898	1.914	1.902
F(000)	1984	1644	1136
T (K)	293(2)	293(2)	293(2)
μ(Mo Kα) (mm^{-1})	5.192	7.359	6.668
index ranges	$-15 \le h \le 23$	$-14 \le h \le 12$	$-10 \le h \le 10$
	$-13 \le k \le 13$	$-18 \le k \le 18$	$-15 \le k \le 8$
	$-29 \le l \le 29$	$-20 \le l \le 20$	$-19 \le l \le 21$
GOF (F^2)	1.001	0.983	1.195
$R_1{}^a$, $wR_2{}^b$ ($I > 2\sigma(I)$)	0.0853, 0.1843	0.0632, 0.1547	0.0558, 0.1283
$R_1{}^a$, $wR_2{}^b$ (all data)	0.1567, 0.2121	0.0932, 0.1675	0.0642, 0.1326

^{a} $R_1 = \sum C| - |F_c/\sum F_o|$. ^{b} $R_2 = [\sum w(F_o - F_c^2)^2/\sum w(F_o^2)]^{1/2}$.

Table 3. Selected Bond Lengths (Å) and Angles (deg) for 3–8

			3				
C(1)−C(3)	1.399(10)	C(2)−C(16)	1.322(10)	C(26)−C(27)	1.262(12)	C(24)−C(35)	1.364(16)
C(52)−N(8)	1.01(2)	C(15)−N(3)	1.143(16)	C(41)−N(1)	1.163(15)	N(9)−C(53)	1.19(3)
C(1)−S(3)	1.735(8)	C(1)−S(1)	1.763(8)				
C(6)−C(3)−C(7)	119.8(6)	C(25)−C(27)−C(22)	116.7(8)				
			4				
Re(1)−C(1)	1.931(13)	Re(1)−C(2)	1.905(14)	Re(1)−C(3)	1.906(11)	Re(1)−N(1)	2.203(9)
Re(1)−N(2)	2.194(9)	Re(1)−Br(1)	2.6240(15)	C(9)−C(15)	1.338(16)	C(16)−C(17)	1.370(19)
N(3)−C(23)	1.152(19)	N(4)−C(20)	1.16(2)				
N(2)−Re(1)−N(1)	83.0(4)	C(3)−Re(1)−Br(1)	175.7(4)	C(2)−Re(1)−N(1)	175.3(4)	C(1)−Re(1)−N(2)	176.9(4)
C(20)−C(19)−C(18)	113.9(14)	C(23)−C(22)−C(21)	107.3(13)				
			5				
Au(1)−P(2)	2.261(8)	Au(2)−P(1)	2.245(8)	Au(1)−Au(2)	3.0861(19)	Au(1)−S(4)	2.316(7)
Au(2)−S(3)	2.323(7)	Au(2)−S(4)	2.862(9)	C(11)−C(12)	1.34(4)	C(13)−C(14)	1.34(4)
P(1)−Au(2)−S(3)	156.5(3)	P(2)−Au(1)−S(4)	176.4(3)	P(2)−Au(1)−Au(2)	120.2(2)	S(3)−Au(2)−Au(1)	89.8(2)
S(4)−Au(1)−Au(2)	62.1(2)						
			6				
Au(1)−P(1)	2.256(3)	Au(1)−S(2)	2.297(3)	Au(2)−P(2)	2.247(3)	Au(2)−S(1)	2.319(3)
Au(2)−S(2)	2.783(3)	Re(1)−N(1)	2.186(9)	Re(1)−N(2)	2.179(9)	Re(1)−Cl(1)	2.464(4)
C(14)−C(15)	1.331(16)	C(16)−C(17)	1.314(15)				
P(1)−Au(1)−S(2)	173.64(12)	P(2)−Au(2)−S(1)	156.91(12)	P(2)−Au(2)−S(2)	117.96(11)	S(1)−Au(2)−S(2)	85.13(10)
N(2)−Re(1)−N(1)	82.8(3)	C(1)−Re(1)−Cl(1)	176.8(4)	C(2)−Re(1)−N(2)	178.6(5)	C(3)−Re(1)−N(1)	173.8(5)
			7				
Pt(1)−N(1)	2.033(7)	Pt(1)−N(2)	2.056(9)	Pt(1)−S(1)	2.264(3)	Pt(1)−S(2)	2.257(3)
C(19)−C(20)	1.292(16)	C(21)−C(22)	1.339(15)	C(19)−S(2)	1.782(13)	C(19)−S(4)	1.765(11)
C(20)−S(1)	1.715(11)	C(20)−S(3)	1.774(11)				
N(1)−Pt(1)−N(2)	80.3(3)	N(1)−Pt(1)−S(2)	170.4(2)	N(2)−Pt(1)−S(2)	97.0(2)	N(1)−Pt(1)−S(1)	93.5(2)
N(2)−Pt(1)−S(1)	169.5(2)	S(2)−Pt(1)−S(1)	90.39(11)				
			8				
Pt(1)−N(1)	2.019(8)	Pt(1)−N(2)	2.032(8)	Pt(1)−S(1)	2.251(3)	Pt(1)−S(2)	2.258(3)
Re(1)−C(33)	1.872(11)	Re(1)−C(34)	1.915(11)	Re(1)−C(35)	1.925(13)	Re(1)−N(3)	2.179(7)
Re(1)−N(4)	2.179(7)	Re(1)−Cl(1)	2.470(3)	C(19)−C(20)	1.283(14)	C(21)−C(22)	1.342(12)
N(1)−Pt(1)−N(2)	78.4(3)	N(1)−Pt(1)−S(1)	94.8(2)	N(2)−Pt(1)−S(1)	173.2(2)	N(1)−Pt(1)−S(2)	173.8(2)
N(2)−Pt(1)−S(2)	96.5(2)	S(1)−Pt(1)−S(2)	90.31(9)	S(1)−Pt(1)−S(2)	90.31(9)	C(34)−Re(1)−N(4)	176.9(4)
C(35)−Re(1)−N(3)	176.3(4)	N(4)−Re(1)−N(3)	83.4(3)	C(33)−Re(1)−Cl(1)	176.5(3)		

after evaporation of the DMF and $CHCl_3$ mixture. Yield: 75 mg (64%). IR (KBr, cm^{-1}): 2017, 1903, 1880 ($\nu_{C\equiv O}$). MS (MALDI-TOF): *m*/*z* 1078.5 $[M - CO]^+$, 794.2 $[M - 3CO - Cl - Re]^+$. Anal. Calcd for $C_{38}H_{39}ClN_5O_4PtReS_4$: C, 38.85; H, 3.35; N, 5.96. Found: C, 38.74; H, 3.29; N, 5.87.

Crystal Structure Determination. The data were collected on a Bruker Smart Apex CCD diffractometer equipped with graphite-monochromated Mo Kα ($\lambda = 0.710\ 73$ Å) radiation using a $\omega-2\theta$ scan mode at 293 K. The highly redundant data sets were reduced using SAINT and corrected for Lorentz and polarization effects. Absorption corrections were applied using SADABS supplied by Bruker. The structure was solved by direct methods and refined by full-matrix least-squares methods on F^2 using SHELXTL-97. All non-hydrogen atoms were found in alternating difference Fourier syntheses and least-squares refinement cycles and, during the final cycles, refined anisotropically. Hydrogen atoms were placed in calculated positions and refined as riding atoms with a uniform value of U_{iso}.

Computational Details. All calculations were carried out with the Gaussian03 programs.[13] We employed the density functional theory (DFT) with no symmetry constraints to investigate the optimized geometries, HOMOs, and LUMOs with the three-parameter hybrid functional (B3LYP).[14] The B3LYP calculations were carried out by the 6-31G* basis set for C, H, O, Cl, Br, P, and S atoms and the effective core potentials (ECP) such as LANL2DZ for Re, Au, and Pt atoms.

Results and Discussions

Synthesis and Characterization. The yellow ligand **3** was prepared by the standard cross-coupling method in the presence of $P(OEt)_3$ and decolored with activated carbon. After deprotecting the biprotected **3** by the alkali $CsOH \cdot H_2O$, the reaction between the resulting dithiolene ligand and $AuPPh_3Cl$ afforded the mononuclear Au(I) complex **5**. It could be purified through column chromatography on alumina. Similarly, the Pt(II) complex **7** was obtained from **3**, by treatment with $CsOH \cdot H_2O$ followed by the addition of $(dbbpy)PtCl_2$. Reaction of $Re(CO)_5X$ ($X = Cl^-$, Br^-) with **3**, **5**, and **7** in toluene gave the respective Re(I) complexes **4**, **6**, and **8** with high yields (Scheme 1). Characterization of all these compounds has been accomplished by IR, ^1H NMR, UV–vis, and mass spectrometry. In IR spectra, the three typical bands found in the CO stretching region for Re(I) complexes are in excellent agreement with the *facial*

(13) Frisch, M. J.; Trucks, G. W.; Schlegel, H. B.; Scuseria, G. E.; Robb, M. A.; Cheeseman, J. R.; Montgomery, J. A., Jr.; Vreven, T.; Kudin, K. N. ; Burant, J. C.; Millam, J. M.; Iyengar, S. S.; Tomasi, J.; Barone, V.; Mennucci, B.; Cossi, M.; Scalmani, G.; Rega, N.; Petersson, G. A.; Nakatsuji, H.; Hada, M.; Ehara, M.; Toyota, K.; Fukuda, R.; Hasegawa, J.; Ishida, M.; Nakajima, T.; Honda, Y. ; Kitao, O.; Nakai, H.; Klene, M.; Li, X.; Knox, J. E.; Hratchian, H. P.; Cross, J. B.; Bakken, V.; Adamo, C.; Jaramillo, J.; Gomperts, R.; Stratmann, R. E.; Yazyev, O.; Austin, A. J.; Cammi, R.; Pomelli, C.; Ochterski, J. W.; Ayala, P. Y.; Morokuma, K.; Voth, G. A.; Salvador, P.; Dannenberg, J. J.; Zakrzewski, V. G.; Dapprich, S.; Daniels, A. D.; Strain, M. C.; Farkas, O.; Malick, D. K.; Rabuck, A. D.; Raghavachari, K.; Foresman, J. B.; Ortiz, J. V.; Cui, Q.; Baboul, A. G.; Clifford, S.; Cioslowski, J.; Stefanov, B. B.; Liu, G.; Liashenko, A.; Piskorz, P.; Komaromi, I.; Martin, R. L.; Fox, D. J.; Keith, T.; Al-Laham, M. A.; Peng, C. Y.; Nanayakkara, A.; Challacombe, M.; Gill, P. M. W.; Johnson, B.; Chen, W.; Wong, M. W.; Gonzalez, C.; Pople, J. A. *Gaussian 03, revision B.04*; Gaussian, Inc.: Wallingford, CT, 2004.

(14) (a) Lee, C.; Yang, W.; Parr, R. G. *Phys. Rev. B* **1988**, *37*, 785. (b) Miehlich, B.; Savin, A.; Stoll, H.; Preuss, H. *Chem. Phys. Lett.* **1989**, *157*, 200.

(15) (a) Caspar, J. V.; Meyer, T. J. *J. Phys. Chem.* **1983**, *87*, 952. (b) Worl, L. A.; Duesing, R.; Chen, P.; Della Ciana, L.; Meyer, T. J. *J. Chem. Soc., Dalton Trans.* **1991**, 849.

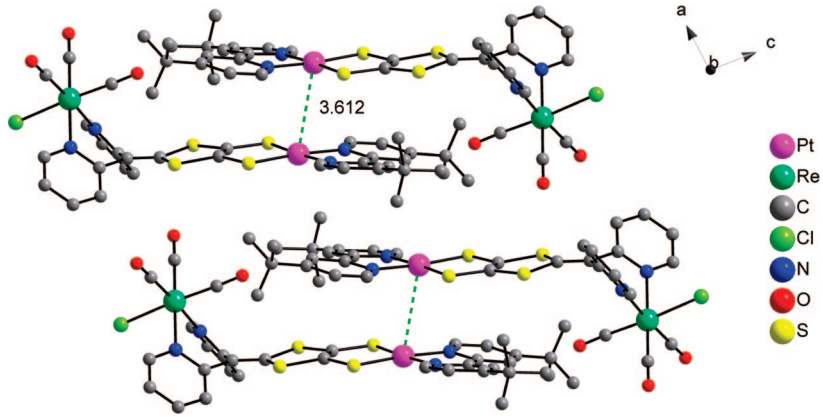

Figure 7. Layered structure of complex **8** viewed along the *b* axis.

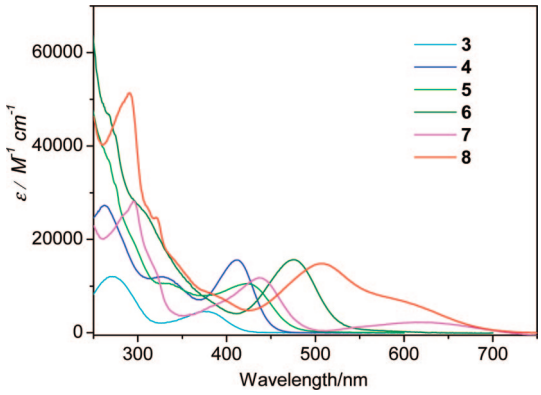

Figure 8. UV–vis absorption spectra of compounds **3**–**8**.

arrangement of the three coordinated C≡O, being consistent with previously reported values.[1,15] All compounds are soluble in most organic solvents and air stable in both fluid solution and solid state.

Crystal Structure Description. The solid structures of compounds **3**–**8** were determined by single-crystal X-ray diffraction. Figures 1–6 show their ORTEP view with atomic numbering, respectively. The crystallographic and data collection parameters are given in Tables 1 and 2; selected bond lengths and angles are listed in Table 3.

For the ligand **3**, two different conformers are present. In both cases, the core of the molecule is rather flat. The atoms of 1,3-dithiole (S1, S3, C1, C2, and C16), one C atom (C3) on the double bond, two S atoms of cyanoethylthio group (S4 and S6), and six atoms on the pyridine ring (N7, C6, C13, C18, C8, and C11) are fairly planar. The other pyridine ring (N6, C7, C17, C4, C21, and C9) deviates from this plane with a dihedral angle of 72.3°. The two cyanoethylthio chains are located on the same side of the main plane. Figure 1b shows a "head-to-head" packing mode along the *b* axis.

For complex **5**, the dihedral angle of the two planes of the pyridine ring is 63.1°. The 1,2-dithiolate ligand bridges the two gold atoms. Each gold(I) center is coordinated to a PPh_3 unit with typical Au−P distances, being 2.245(8) Å for Au(2)−P(1) and 2.261(8) Å for Au(1)−P(2). The atom Au(1) adopts a typical linear coordination mode with a bond angle of 176.4(3)° (P(2)−Au(1)−S(4)), while the angle at Au(2) (P(1)−Au(2)−S(3), 156.5(3)°) deviates from linearity. The intramolecular contact of Au(1)−Au(2) is 3.0861(1) Å, which is very similar to those found for other gold dithiolate complexes, $[Au_2(\mu\text{-MNT})(PPh_3)_2]$[16a] (3.115(3) Å), $[Au_2(3,4\text{-}S_2C_6H_3CH_3)(PPh_3)_2]$[16b] (3.096(2) Å), and $[Au_2(\mu\text{-dmit})(PPh_3)_2]$[16c] (3.068(1) Å). The shorter Au−S distances (S(3)−Au(2), 2.323(7) Å; S(4)−Au(1), 2.316(7) Å) are also within the normal range.

Similar to that in compound **5**, the two pyridine rings in **7** are not coplanar, with an interplanar angle of 113.8° (Figure 3). The central Pt(II) adopts a slightly distorted square-planar coordination geometry. The chelating dbbpy ligand results in an N−Pt−N bond angle of 80.3(3)°, which is significantly less than the idealized value of 90°. The average Pt−N distance of 2.045(3) Å is within the range of those for other platinum polypyridine complexes.[17a–d] As shown in the packing diagram for **7** in Figure S2, the structure consists of columns of molecules along the *b* direction.

The rhenium atoms of all Re(I) complexes (**4**, **6**, and **8**) are in a distorted octahedral coordination environment with three carbonyl ligands in a *fac* arrangement, two N atoms from two pyridine rings of the ligand, and a halogen atom. Six-menbered rings formed by the bidentate bis(2-pyridyl) group and the Re atoms are in a boat conformation, orienting away from the central C−C double bonds. The N−Re−N angles are 83.0(4)° for **4**, 82.8(3)° for **6**, and 83.4(3)° for **8**, which are all less than 90°. Solvated molecules are found in complexes **4** (two $CHCl_3$), **6** (two CH_2Cl_2), and **8** (one DMF). Compared to **3**, the molecule of **4** is somewhat bent. The crystal packing for **6** viewed along the *a* axis is shown in Figure S3. There is no intramolecular

Table 4. Electronic Absorption and Luminescence Data for Compounds 3–8 at 298 K

	absorption	luminescence	
compound	λ_{abs}/nm (ϵ/M^{-1} cm^{-1})	λ_{ex}/nm	λ_{em}/nm
3	271 (12 100), 377 (5000)	423 (CH_2Cl_2)	455
4	262 (27 300), 329 sh (12 000), 411(15 600)	439 (CH_2Cl_2)	530
		362 (solid)	494
5	290 sh (21 500), 329 sh (10 600), 422 (10 500)	396 (CH_2Cl_2)	468
6	300 sh (27 500), 475 (15 600)	468 (CH_2Cl_2)	597
		393 (solid)	560
7	295 (28 200), 437 (11 800), 620 (2 200)		
8	290 (51 300), 507 (14 800), 600 sh (6700)		

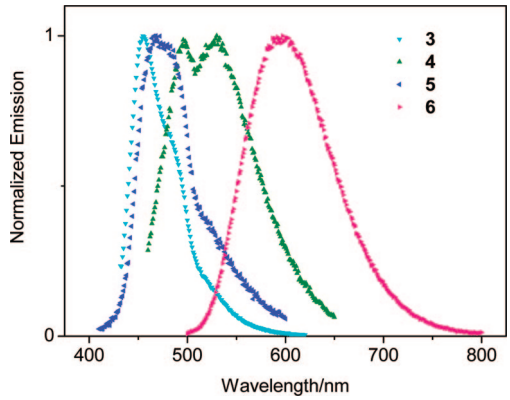

Figure 9. Normalized fluorescence spectra of **3**–**6** in CH_2Cl_2 solution at 298 K.

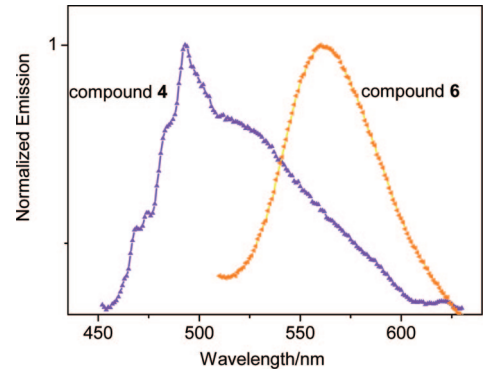

Figure 10. Normalized emission spectra of compounds **4** and **6** in the solid state at 298 K.

shorter contact between Au(1) and Au(2) because of the large distance (3.747 Å). Complex **8** crystallizes in the $P\bar{1}$ triclinic space group. In comparison, the structure of **8** is less distorted than **7** in the square plane around the Pt center. The S−Pt−S angle (90.31(9)°) is similar to that in compound **7** (90.39(1)°). The molecules are stacked in a head-to-tail arrangement as shown in Figure 6. The nearest Pt···Pt distance is 3.612 Å, and the neighboring molecules are arranged as a "dimer" along the *b* axis (Figure 7). No obvious intermolecular Pt···S or S···S interaction was detected in these crystal structures.

Electronic Absorption and Luminescence Properties. The UV–vis absorptions of compounds **3**–**8** in CH_2Cl_2 solution are shown in Figure 8, and their spectral data are given in Table 4. For the ligand **3**, the absorption peaks at 271 and 377 nm come from the $\pi-\pi^*$ transitions. All complexes **4**–**8** display intense absorption bands at ca. 250–305 nm in CH_2Cl_2 with extinction coefficients on the order of 10^4 M^{-1} cm^{-1}, which can be also assigned to spin-allowed intraligand ($\pi-\pi^*$) transitions. The absorption peaks at 422 nm for **5** and 437 nm for **7** are assigned to dπ(Au)−π^*(BPyDT) and dπ(Pt)−π^*(BPyDT) MLCT transitions, respectively. Furthermore, there is a broad absorption band around 620 nm ($\epsilon = 2200$ M^{-1} cm^{-1}) for **7**. This absorption is presumably attributed to the interligand charge transfer, which is often observed in Pt(NN)(SS) systems.[17a,b,e] The absorptions at 410–570 nm for complexes **4**, **6**, and **8** are due to the dπ(Re)−π^*(ligand) transitions, which are typical for Re(I) polypyridine complexes. Compared to the low-energy MLCT transition in **5**, the relative absorption band is red-shifted in **6**. This implies that the coordination of **5** to the Re(I) center reduces the transition energy and thus changes the absorption.

Upon photoexcitation, compounds **3**–**6** exhibited blue to red luminescence in CH_2Cl_2 solutions under ambient conditions. Their emission spectra are shown in Figure 9, and the data are also listed in Table 4. The blue fluorescent emission (455 nm) of **3** is attributed to $\pi^*-\pi$ relaxation. Excited at 423 nm, the emission maxima are positioned at 496 and 530 nm for **4**; compared to **3**, the red shift of the emission band is a result of the coordination to the Re atom. With the substitution of $-CH_2CH_2CN$ by $AuPPh_3$, complex **5** has a lower emission energy (468 nm) than **3**, which could be ascribed to the effect of the electron-rich $AuPPh_3$ units.[16a,18] The photoluminescence spectrum in **6** centered at 597 nm in CH_2Cl_2 solution at room temperature is characteristic of Re(I)-based ^{3}MLCT emission frequently found in $ReL(CO)_3Cl$ (L = polypyridine) complexes. We note that the high-energy emission in **6** at around 510–540 nm overlaps with the luminescence observed from compound **5** when excited at 396 nm. This overlap may be interpreted as a Au-contained ligand-localized contribution.[4a] Compared with mononuclear complex **4**, the emission maximum of the trinuclear **6** is significantly red-shifted (ca. 70 nm). Intense luminescence has been observed for both **4** and **6** in the solid state, with the emission maxima shifting ca. 37 nm to the high-energy region relative to those in fluid solution (Figure 10). No luminescence was detected for complexes **7** and **8** in both the solid and solution state, which may be attributed to the nonradiative thermal deactivation in the Pt(II)-containing complexes.[17a,19]

Computational Studies. Figure 11 shows the graphical representation of HOMOs and LUMOs for ground states of **3**−**8**. Table 5 summarizes the calculated molecular orbital energies and energy gaps. Table 6 gives the electron distribution for comparison.

The values of the calculated energy gaps match well with the UV–vis spectroscopic data, cf. Table 5. The energy gaps of HOMO to LUMO are 3.887, 3.415, 2.755, and 2.971 eV for compounds **3**–**6**, respectively, which correlate to the MLCT absorption maxima. Comparatively, the calculated energy gaps between the HOMO and LUMO for **7** and **8** are relatively small (less than 1.800 eV), while the energy gaps from HOMO-1 to the LUMO level are close to 2.500 eV. Compound **7** shows MLCT transitions at 437 and 620 nm occurring from the HOMO-1 to the LUMO level and the HOMO to LUMO level, respectively. The calculated energy gaps |HOMO-1−LUMO| and |HOMO–LUMO| for complex **8** are responsible for the respective absorption bands at 507 and 600 nm.

As shown in Table 6 and Figure 11, the electron distributions on LUMO, HOMO, and HOMO-1 of molecule **3** are located on the $BPyDTS_2$ moiety (more than 95.0%), with the cyanoethyl groups almost empty. Complex **4** shows that the LUMO mainly consists of $\pi^*(BPyDTS_2)$ character (92.6%) resulting from the overlap of pyridine rings and the sulfur-included heteroatom ring, while the HOMO contains 20.4% dπ(Re) character, with 33.3% electron density located on Br^-, 34.1% on the $BPyDTS_2$ segment, and the remainder on π(C≡O).

(16) (a) Dávila, R. M.; Elduque, A.; Grant, T.; Staples, R. J.; Fackler, J. P., Jr *Inorg. Chem.* **1993**, *32*, 1749. (b) Gimeno, M. C.; Jones, P. G.; Laguna, A.; Laguna, M.; Terroba, R. *Inorg. Chem.* **1994**, *33*, 3932. (c) Cerrada, E.; Jones, P. G.; Laguna, A.; Laguna, M. *Inorg. Chem.* **1996**, *35*, 2995.

(17) (a) Bevilacqua, J. M.; Eisenberg, R. *Inorg. Chem.* **1994**, *33*, 2913. (b) Chen, C. T.; Liao, S. Y.; Lin, K. J.; Chen, C. H. *Inorg. Chem.* **1999**, *38*, 2734. (c) Zuo, J. L.; Xiong, R. G.; You, X. Z.; Huang, X. Y. *Inorg. Chim. Acta* **1995**, *237*, 177. (d) Pap, J. S.; Benedito, F. L.; Bothe, E.; Bill, E.; DeBeer George, S.; Weyhermüller, T.; Wieghardt, K. *Inorg. Chem.* **2007**, *46*, 4187. (e) Cummings, S. D.; Eisenberg, R. *J. Am. Chem. Soc.* **1996**, *118*, 1949.

(18) King, C.; Wang, J. C.; Khan, Md. N. I.; Fackler, J. P., Jr *Inorg. Chem.* **1989**, *28*, 2145.

(19) (a) Kunkely, H.; Vogler, A. *J. Am. Chem. Soc.* **1990**, *112*, 5625. (b) Barigelletti, F.; Sandrini, D.; Maestri, M.; Balzani, V.; von Zelewsky, A.; Chassot, L.; Jolliet, P.; Maeder, U. *Inorg. Chem.* **1988**, *27*, 3644.

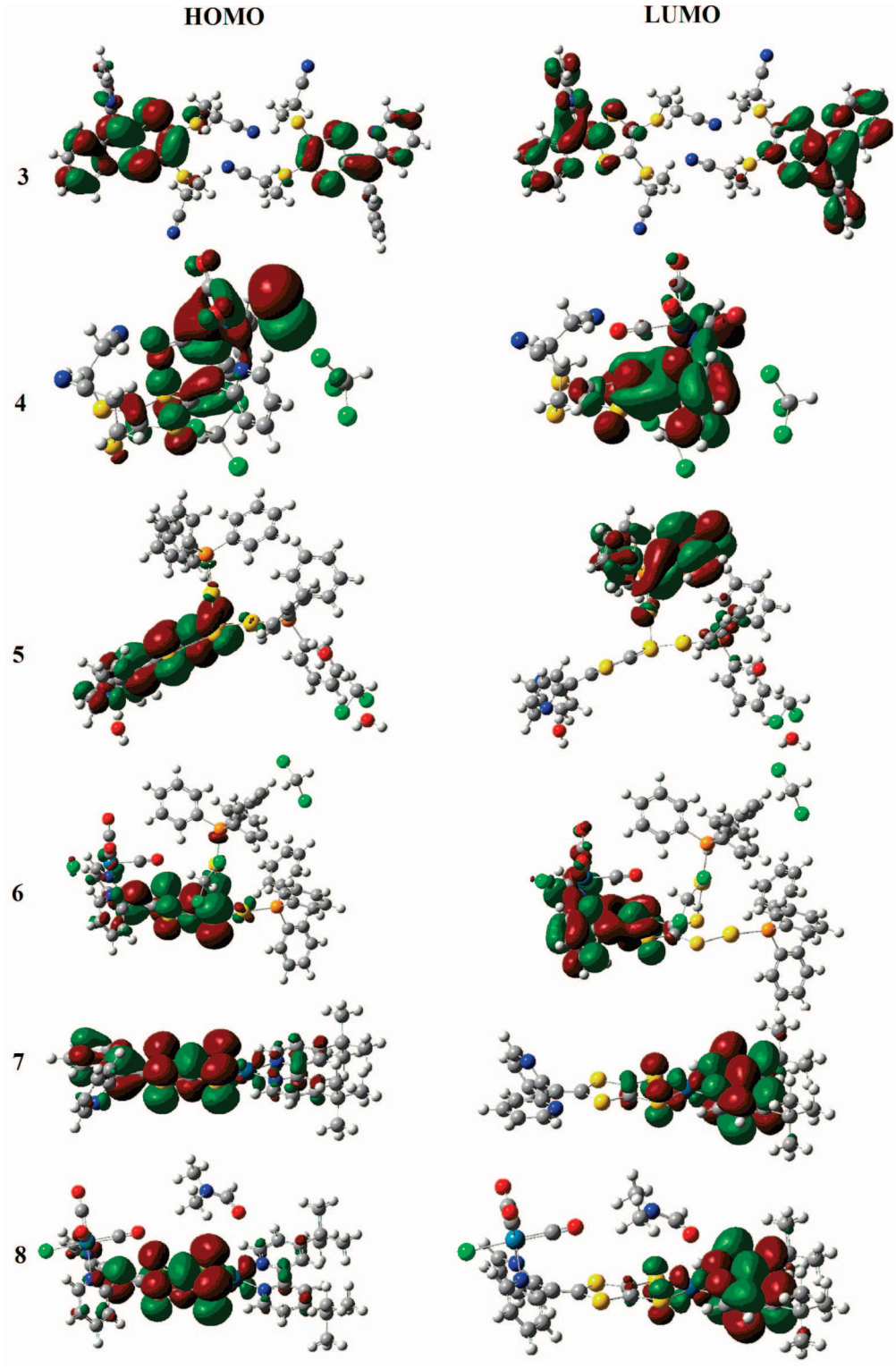

Figure 11. Graphical representation of HOMO and LUMO diagrams for **3–8**.

Table 5. Calculated Molecular Orbital Energies (eV) for 3–8

compound	HOMO-1 (au)	HOMO (au)	LUMO (au)	|HOMO–LUMO| (eV)	|HOMO-1−LUMO| (eV)	exptl[b] (eV)
3	−0.19475[a]	−0.19475[a]	−0.05187	3.887	3.887[a]	3.288
4	−0.21525	−0.21326	−0.08776	3.415	3.469	3.016
5	−0.19096	−0.15026	−0.04901	2.755	3.862	2.938
6	−0.19647	−0.16920	−0.06001	2.971	3.713	2.610
7	−0.18504	−0.14263	−0.09353	1.336	2.490	2.000,[c] 2.837[d]
8	−0.18823	−0.16023	−0.09640	1.737	2.499	2.066,[e] 2.445[f]

[a] HOMO-1 and HOMO are degenerate. [b] Determined from UV–vis absorption spectra. [c] Absorption at 620 nm used. [d] Absorption at 437 nm used. [e] Absorption at 600 nm used. [f] Absorption at 507 nm used.

Table 6. Percentage Composition (%) of Calculated Molecular Obital

		composition %					
compound		Re	Br	CO	$BPyDTS_2$		
3	LUMO	-[a]	-[a]	-[a]	95.8		
	HOMO	-[a]	-[a]	-[a]	96.6		
4	LUMO	2.4	-[b]	2.5	92.6		
	HOMO	20.4	33.3	8.2	34.1		
		Re	Cl	CO	$BPyDTS_2$	Au	PPh_3
5	LUMO	-[a]	-[a]	-[a]	1.2	7.0	91.8
	HOMO	-[a]	-[a]	-[a]	92.2	4.3	3.4
6	LUMO	2.9	-[b]	3.1	92.0	-[b]	-[b]
	HOMO	1.3	-[b]	-[b]	84.5	6.4	3.6
		Re	Cl	CO	$BPyDTS_2$	Pt	dbbpy
7	LUMO	-[a]	-[a]	-[a]	8.2	6.3	85.5
	HOMO	-[a]	-[a]	-[a]	90.2	2.4	7.4
8	LUMO	-[b]	-[b]	-[b]	5.2	5.7	88.9
	HOMO	1.0	-[b]	-[b]	88.4	4.3	4.8

[a] Atoms not included in the molecule. [b] Percentage composition of less than 1%.

For complex **5**, the LUMO is dominated by the $AuPPh_3$ group, while the HOMO is centered on the $BPyDTS_2$ moiety. The LUMO of molecule **6** is similar to that of **4**, which is dominated by $BPyDTS_2$ (92.0%), with an almost equal distribution (ca. 3%) on Re and C≡O. However, the HOMO of **6** is quite different from that of **4**: most of the electron density (84.5%) is distributed on $BPyDTS_2$, with ca. 10% located on the $AuPPh_3$− ligand. This difference is reflected in the distinction of the UV–vis absorption. It could also be the reason for the photoluminescence variation (the emission is 530 nm for **4** and 597 nm for **6** in solution).

The electron density of **7** is mainly located on Pt(dbbpy) at the LUMO level and on $BPyDTS_2$ at the HOMO level. For complex **8**, it is almost the same as **7**, except only 1.0% of electron distribution on the rhenium atom is contained at the HOMO level. These HOMO and LUMO distributions for **7** and **8** support the assignments of the absorption and are consistent with previous reports on related complexes.[4b,17a,19]

In conclusion, our results demonstrate that the new polypyridine ligand containing coupled bis(2-pyridyl) and extended 1,2-dithiolene is a versatile bridge for heteronuclear complexes. Based on the new ligand, tricarbonyl rhenium(I) heterotrinuclear complex **6** and heterodinuclear complex **8**, and their precursor di- and mononuclear compounds, have been prepared and structurally characterized. The protected ligand **3** and metal complexes **4**–**6** exhibit blue to red luminescence in CH_2Cl_2 solution under ambient conditions. The ground-state structures for all the compounds have been investigated by DFT calculations.

Acknowledgment. This work was supported by the Major State Basic Research Development Program (2006CB806104 and 2007CB925103), the National Science Fund for Distinguished Young Scholars of China (Grant 20725104), and the National Natural Science Foundation of China (Grant 20531040).

Supporting Information Available: Crystallographic data for compounds **3**–**8** in CIF format; Cartesian coordinates in DFT calculations and the optimized geometries for **3**–**8**; packing diagram of compounds **6** and **7**. This material is available free of charge via the Internet at http://pubs.acs.org.

OM700776S